DYNAMIC FRACTURE MECHANICS ANALYSIS OF HYDROGEN EMBRITTLEMENT OF Zr-2.5 Nb PRESSURE TUBE

Y. FUKUDA, S. KUSUMOTO, S. USAMI

Hitachi Research Laboratory, Hitachi Ltd., 4026 Kuji-Machi, Hitachi-Shi, Ibaraki-ken, 319-12, Japan

E. SHIBATO

Hitachi Works, Hitachi Ltd., 3-1-1 Saiwai-cho, Hitachi-shi, Ibaraki-ken, 317, Japan

K. HAYASHI

Power Reactor and Nuclear Fuel Development Corporation, 1-9-13 Akasaka, Minato-ku, Tokyo, 107, Japan

SUMMARY

This paper describes the dynamic fracture behavior of heat treated Zr-2.5 Nb pressure tube which is used for the Prototype Heavy Water Reactor "FUGEN" that is under construction by the Power Reactor and Nuclear Fuel Development Corporation.

Hydrogen is picked up by the reactor pressure tube from the water coolant. The hydrogen concentrates in regions with stress concentration and the regions become very brittle. Therefore, in designing structures and safety systems, the effects of stress on hydrogen density and hydrogen concentration must be taken into consideration. When a local fracture initiates in a brittle region it must be arrested in order to prevent unstable fracture of the pressure tube.

A basic study of fatigue crack growth and static fracture toughness has been reported at the second SMIRT Conference, Berlin 1973.

We have done four experiments in order to clarify the dynamic fracture behaviors of the pressure tubes. The experiments are: (1) a leak before rupture experiment using tube specimens with a part-through-crack under internal repeated pressure, (2) a dynamic fracture toughness experiment using drop weight equipment at temperature to 300 ℃, (3) a crack arrest experiment using a double cantilever tube specimen under wedge force, and (4) a hydrogen enrichment and concentration experiment with the specimen subjected to various stresses.

The main results of these experiments when the concentration of hydrogen is 300 ppm, which is higher than the concentration after 30 years of plant operation, are summarized as follows:

(1) The failure mode of a tube with detectable flaws is leak-before-rupture for design stress. The critical flaw lengths of leak-before-rupture under design stress are the value of 50 mm at 300 ℃ and the value of 10 mm at room temperature.

(2) Dynamic fracture toughness is a little smaller than static fracture toughness and is nearly equal to crack arrest toughness. Dynamic fracture toughness (at $\dot{K} = 10^6$ kg/mm$^{3/2}$ sec^{-1}) is 55 kg/mm$^{3/2}$ at room temperature and is about 180 kg/mm$^{3/2}$ at 300 ℃.

(3) Static fracture toughness is greatly affected by stress during hydrogen enrichment and equals the dynamic fracture toughness of a tube free from stress during hydrogen enrichment.

These test results are discussed systematically from the view of dynamic fracture mechanics.

The conclusion which we obtained is that the pressure tubes with detectable flaws might be used safely, even if they are irradiated with coolant water at 300 ℃ and then stressed at room temperature.

1. Introduction

The Power Reactor and Nuclear Fuel Development Corporation has been developing a prototype reactor, "FUGEN", heavy water moderated and light water bioling cooled, and has decided to adopt Zr-2.5Nb as the pressure tube material because of its good nuclear characteristics and its high mechanical strength. However, hydrogen picked up from coolant water reportedly lead to embrittlement of pressure tubes.

When a flawed tube, under tensile stress, is covered with water, hydrogen picked up from the water by the tube becomes Zrconium-hydride. Zrconium-hydride molecules gather in groups and these groups arrange themselves parallel to the longitudinal direction of a flaw, in a local region around the flaw tip, which weakens the Zr-25Nb. If a local brittle fracture should then occur near the flaw tip, and if the growth of the fracture is not stopped, then it may grow and become a catastrophic fracture.

Basic studies of fatigue crack growth and static fracture toughness have been reported in the literature (KUSUMOTO[1]), but very few studies of dynamic fracture toughness or crack arrest toughness have been reported for Zr-2.5Nb.

We planned out program to study the dynamic fracture behavior of this material, i.e., the dynamic fracture, crack arrest and static fracture toughness of a material with local brittle regions around flaws.

2. Experimental Techniques

2.1 Material

The material investigated is aged extruded tube made from Zr-2.5Nb, and satisfying the specifications for reactor pressure tube. The heat treatment consisted of water quenching from 870°C, cold drawing until reduced 10 ~ 15% and then aging by holding at 500°C in a vacuum for 24h. Tube dimensions are 117.8 mm in inside diameter and 4.3 mm in wall thickness. Four kinds of specimen were prepared, differing in hydrogen content, 5 (as received), 50, 100 and 250 ppm. Hydrogen was charged by the following methods: a 800 mm long piece was shot blasted on the surface and heated at 450 ~ 500°C in hydrogen gas for a hours.

Table 1 shows the circumferential mechanical properties of the material measured by the ring tensile test using 6.4 mm wide ring pieces (KIMURA [2]). The effects of hydrogen content on the mechanical properties are not so prominent.

2.2 Bending Test

A special bending test was developed as one step in the development of a method for surveillance of reactor pressure tubes.

A crescent-shaped specimen was 75 mm long 30 mm wide and 4.3 mm thick, was cut from the pressure tube. A sharp notch cut at the middle of one 75 mm edge. As shown in Fig. 1, the specimen is set at both ends on a jig, inclined by 13.5° from the load axis to avoid out of plane bending at the notch area.

A pulsating bending load was applied to the specimen to generate a fatigue crack at the root of the notch by three points bending. Afterwards, the static or dynamic bending force was increased until the specimen fractured to obtain a value for fracture toughness.

2.3 Dynamic fracture toughness test

A dynamic load is applied to the bending specimen by equipment which can drop a weight of 25 kg from a height of 0 ~ 6 m. Dynamic load is measured by strain gauges mounted near the crack tip and the edge of the drop weight. Tow impact strain waves from the gauges are shown in figure 2. The edge mounted strain gauge could not be used because the elastic vibrations resulting from a drop weight edge masked the moment of fracture. Therefore the strain gauge mounted near the crack tip was used in all dynamic tests. Dynamic strain which corresponds to dynamic load, is measured by using two differential amplifiers designed for high frequencies. The out put of the amplifiers is first recorded on a transient recorder, which consists of a 1000 W semiconductor memory and has a 2×10^{-6} second resolution time. The strain measurment method is shown in figure 3. In the high temperature test, specimens are heated by thermal conduction from steel blocks which are heated by electric heaters wound around them. A strain is converted into a load with a calibration curve which is drawn with data obtained on the relation between load and strain which is obtained in static load tests.

2.4 Method of hydrogen enrichment under applied stress

Two kinds of specimen are hydrogen enriched. One is a specimen with a fatigue crack and the other a specimen with a slit cut with a saw. Both types of specimen are set in a loading frame like the one shown in figure 4. Applied load is measured with two specimen mounted strain gauges, which are calibrated with a testing machine. Assembles are put into a chamber and then held in a hydrogen atomosphere at $500^{\circ}C$ for 30 to 140 min. in order to enrich them. After hydrogen enrichment, the applied load is measured with strain gauges again. The result is that the load after enrichment decreases by 15 percent of the initial load. The hydrogen content of a specimen in measured by vaporization.

2.5 Crack arrest toughness test

The tube specimens used in the crack arrest toughness test are similar to DCB specimen. Each specimen has two axial quide grooves cut along its inner surface and test net sections 2 mm thick. The construction of an assembly is shown in figure 5. Deflection is constant because a screw is used to apply the force that is needed to open a crack, and the stress intensity factor decreases as a brittle crack propagates. Brittle crack propagation velocity is measured with crack gauges mounted at the front of a crack tip. A crack gauge has a 25 mm gauge length and a sensitivity of 80μ strain/mm. Three or four sheets of crack gauges are mounted close to each other on one side of a specimen. The out put from crack gauges is memorized by transient recorder and is fed to a pen recorder in the same manner as in the dynamic fracture toughness test.

3. Results and discussion

3.1 Stress intensity factor and fracture toughness

Stress intensity factor, K is used for data arrengement because fracture stress in the present test is, in many cases, small enough to allow the use of linear fracture mechanics. The stress intensity factor for three point bending specimens is given by the following equation (BROWN & SRAWLEY[3])

$$K = \sigma_n \cdot \sqrt{a} \left\{ \left(1-\frac{a}{H}\right)^2 \left[1.93 - 3.07\left(\frac{a}{H}\right) + 14.53\left(\frac{a}{H}\right)^2 - 25.11\left(\frac{a}{H}\right)^3 + 25.80\left(\frac{a}{H}\right)^4 \right] \right\} \quad (1)$$

where,

a : crack length

σ_n : net section stress

H : width of specimen

The net section stress, σ_n is as follows

$$\sigma_n = \frac{6}{4} \cdot \frac{P \cdot L}{T(H-a)^2} \cdot \frac{1}{\cos\theta} \quad (2)$$

where

P : applied load

L : span between the two supporting points

T : thickness

θ : inclination angle

It is difficult to calculate the stress intensity factor for the tube specimen used in the crack arrest test because a thin half cylinder cross section has a stiffness which varies complexly as cracks propagate. Because of the similarity of the test and DCB specimens, the following modified stress intensity factor equation was used (GALLAGHER [4])

$$K = \frac{2\sqrt{3}}{H'^{\frac{3}{2}}} \cdot P' a \left\{ 1 + 0.7\left(\frac{H'}{a}\right) \right\} \quad (3)$$

where

a : crack length

P′ : applied load a unit thickness

H′ : equivalent width

From eq.(3), stress intensity factor is proportional to applied load when crack length is constant. Therefore, the crack arrest toughness of a tube with a hydrogen content of 280 ppm is obtained by multiplying the ratio crack arrest load, Pa,/crack initiate load, Pi, by the static fracture toughness, Kc, for a hydrogen content of 280 ppm.

$$Ka_{(280ppm)} = Kc_{(280ppm)} \times \left. \frac{Pa_{(280ppm)}}{Pi_{(280ppm)}} \right|_{a=const.} \quad (4)$$

In the case of a specimen with a different hydrogen content, crack arrest toughness, $Ka_{(H_2)}$ is as follows

$$Ka_{(H_2)} = Ka_{(280ppm)} \times \left. \frac{Pa_{(H_2)}}{Pa_{(280ppm)}} \right|_{a=const.} \quad (5)$$

3.2 Dynamic fracture behavior

3.2.1 Dynamic fracture toughness

In order to study the effect of the stress intensity factor increase rate, $\dot{K}$, the hydrogen content, H_2, and the temperature, T, on dynamic fracture toughness, Kd, a dynamic fracture test is carried out. The effect of $\dot{K}$ on Kd is shown in figure 6. $\dot{K}$ is calculated using the slope of a load-time curve, a typical example of which is shown in figure 7, just prior to brittle fracture. Kd decreases as $\dot{K}$ increases, while above $\dot{K} = 10^4$ $kg/mm^{\frac{3}{2}} \cdot sec^{-1}$, Kd is almost constant and below $\dot{K} = 10$ $kg/mm^{\frac{3}{2}}$ sec^{-1}, Kd is considerablly dependent on $\dot{K}$. The ratio of dynamic fracture toughness, Kd, at $\dot{K} = 10^{-6}$ $kg/mm^{\frac{3}{2}} \cdot sec^{-1}$, to static fracture toughness, Kc, is 0.73, 0.78 and 0.42, when the hydrogen content is 300, 200, and 5 ppm respectively.

The effect of the hydrogen content, H_2 on Kd is shown in figure 8. The ratio of Kd to Kc decreases considerablly as the hydrogen content decreases. The reason for this seems to be that the ductility of a material with a low hydrogen content is excellent, and therefore the degree to which ductility is decreased by the constraints of plastic flow under a dynamic load is large in comparison with a material with a high hydrogen content.

The effect of temperature on Kd ($\dot{K} = 10^5 \sim 10^6$ $kg/mm^{\frac{3}{2}} \cdot sec^{-1}$) is shown in figure 9. Kd increases slowly with increasing temperature but not as much as Kc does. At 280°C, Kd is, in the same way that Kc is, almost unrelated hydrogen content. The ratio of Kd ($\dot{K} = 10^5 \sim 10^6$ $kg/mm^{\frac{3}{2}} \cdot sec^{-1}$) to Kc is about 0.8 at 280°C.

The static fracture toughness of specimens containing 5 ppm hydrogen is almost the same at room temperature and at 280°C, but the dynamic fracture toughness is not. Though no reason for this can be found, observation of the fracture surfaces lends support to the calculated results, because the fracture surfaces of the room temperature specimens are more brittle than those of the 280°C specimens, as shown in figure 10.

3.2.2 Fracture Toughness of hydrogen enriched specimen under applied stress

The brittle fracture behavior of specimens that are cut from a tube, fatigue cracked or notched and then hydrogen enriched while under stress is very different from that of specimens that are cut from a tube and fatigue cracked or notched after the tube is hydrogen enriched in a stress free enviroment. The latter type of specimen is used in the dynamic fracture and crack arrest tests describeded in this paper.

Using a test machine with ordinary compliance, hydrogen enriched specimens under applied stress do not fracture at once and brittle cracks stop propagating to some extent. When the deflection of the loading point is contanuously in creased, a brittle crack propagates in steps in which crack length and time are related. The fracture toughness of hydrogen enriched specimens under applied stress is calculated with the load of the third or fourth step, because crack length at those steps is from 0.5 to 1.0 mm, which is large enough to be considered a crack in the engineering sense. Next, at the fourth or fifth steps, a crack propagates so extensively that the specimen is considered fractured.

Figure 11 shows the relation between the fracture toughness of a specimen with a fatigue crack and one with a saw-cut notch, and the stress applied in the hydrogen enriching treatment. The hydrogen content of specimens is about 200 ppm. The smaller the applied stress is the larger the effect of the notch root configuration. In the case where applied stress is above 5 kg/mm^2, there is no difference between the fracture toughness of saw-cut notch specimens and fatigue-crack specimens. The reason for this is that in the case of hydrogen enrichment under applied stress, Zirconium-hydride molecules gather in groups and these groups arrange them selves parallel to the direction of advance of a crack, which is perpendicular to the direction of tensile stress. This region of Zirconium-hydride molecule groups is very brittle, but the brittleness decreases sharply with increasing distance from the crack tip, in the same way that stress distribution decreases with increasing distance from a crack tip. . This distribution of static fracture and crack arrest toughness, Kc and Ka, respectively, in front of a crack tip is relatively easy to model, as shown in figure 12. In this case, since static fracture toughness, Kc, near the crack tip in creases sharply with increasing distance from the tip and since is larger than crack arrest toughness, Ka, no large scale final fracture occurs until two or three small scale fractures have occured. In a region where a large scale fracture is initiated, the effect of notch root configuration on fracture is negligible.

Figure 13 shows the fracture surface appearance of fracture toughness tested specimens. The difference in specimens enriched under stress and those not so enriched is very large.

3.2.3 Crack arrest toughness

It is very difficult to obtain an absolute value for crack arrest toughness, Ka because specimen configuration is very complicated. Therefore, crack arrest toughness is calculated from crack arrest load using eq.(4) ~ (5) in the previous section. The results of the crack arrest test, expressed as the relation between crack arrest load and crack length, are shown figure 14. The crack arrest length of a crack is not the same for both sides of a specimen. Crack length in figure 14 represents the average of the crack arrest lengths of cracks on both sides of the specimens. The variation in load at crack arrest seems to results from the difference in right and left side crack length. From figure 14, the ratios of the crack arrest loads of speciren containing 5 ppm, 65 ppm and 120 ppm hydrogen to the load of a specimen containing 280 ppm are 1.97, 1.65 and 1.48 respectively. The ratio of crack arrest load to crack initiate load in a specimen containing 280 ppm hydrogen is almost 0.8 and the static fracture toughness, Kc is 75 $kg/mm^{\frac{3}{2}}$. Therefore crock arrest toughness, Ka of the tube specimen containing 5, 65, 120 and 280 ppm hydrogen is 118, 99, 89 and 60 $kg/mm^{\frac{3}{2}}$ respectively. Figure 15 shows a typical example of brittle crack propagation behavior in which crack length is related to propagation. It can be seen from this figure, that crack propagation velocity is nearly constant until just before a crack stops propagating. Average crack propagation velocity in the present tests ranged from 33 to 102 m/sec. and is almost equal to that for steel (CROSLEY [5])

3.2.4 Relation among Kc, Kd and Ka

The static fracture, dynamic fracture, and crack arrest toughness, Kc, Kd and Ka, respectively, of specimens fatigue cracked after hydrogen enrichment and the Kc' of specimens hydro gen enriched under applied stress after fatigue cracking are summarized in figure 16. Values for Kc are considerablly higher than those for Kc' specially in the region of small hydrogen content. K'c is nearly equal to Ka. This means that, in the case of hydrogen enrichment under applied stress, a fracture occurs at a crack tip as shown in figure 14, and therefore, in designing pressure tube in the viewpoint of fracture mechanics, it is necessary to consider crack arrest rather than static fracture toughness.

Values for dynamic fracture toughness, Kd, ($\dot{K} \simeq 10^5 \sim 10^6$ $kg/mm^{\frac{3}{2}} \cdot sec^{-1}$) are a little lower than those for crack arrest toughneos, Ka, (crack velocity $\simeq 33 \sim$ 100 m/sec).

Therefore, when Ka is unknown, dynamic fracture toughness can be used in stead of crack arest toughness.

4. Conclusions

(1) Dynamic fracture toughness at room temperature decreases with increase in the rate of the stress intensity factor, and above $\dot{K} = 10^5$ kg/mm$^{\frac{3}{2}}$ $\cdot$ sec^{-1}, it converges to a certain value depending on the hydrogen content of the specimen

(2) The ratio of dynamic fracture (above $\dot{K} = 10^5$ kg/mm$^{\frac{3}{2}}\cdot$ sec^{-1}) to static fracture toughness becomes larger as the hydrogen content increases (These values are 0.42, 0.78 and 0.73 for 5, 200 and 300 ppm hydrogen content respectively.)

(3) Material with 300 ppm of hydrogen has the same dynamic fracture toughness ($\dot{K} = 10^5 \sim 10^6$ kg/mm$^{\frac{3}{2}}\cdot$ sec^{-1}) as that of material with 5 ppm at 280°C

(4) The fracture toughness of specimens hydrogen enriched under applied stress is greatly affected by stress, but this saturates above a certain value (15 kg/mm$^{\frac{3}{2}}$ of stress intensity factor).

(5) The fracture toughness in (4) is nearly equal to crack arrest toughness, which is obtained in a crack arrest test of tube specimens. (These values are 118, 99, 89 and 60 kg/mm$^{\frac{3}{2}}$ for 5, 65, 120 and 280 ppm of hydrogen respectively.)

(6) The values obtained for dynamic fracture toughness (above $\dot{K} = 10^5$ kg/mm$^{\frac{3}{2}}$ $\cdot$ sec^{-1}) are a little smaller than those obtained for crack arrest toughness, except for the values obtained near $\dot{K} = 10^3$ kg/mm$^{\frac{3}{2}}$ $\cdot$ sec^{-1}, which are nearly equal to those for crack arrest toughness.

Reference

1 KUSUMOT, S, et al, "Effects of Hydrogen Content, Temperature and Crack Configuration on Fatigue Crack Propagation and Unstable Fracture Behavior of Zr-2.5Nb Pressure Tube", Second Intl. Conf. on Structural Mechanics in Reactor Technology, Berlin, September 10-14, 1973.

2 KIMURA, K., et al., Report of Japan Power Reactor and Nuclear Fuel Development Corp. No. SJ 355 71-01, 1972

3 BROWN, W.F, SRAWIEY, J.E., "Plane Strain Crack Toughness Testing of High Strength Metallic Materials" ASTM STP 410, 1967

4 GALLAGHER, J., "Experimentally Determined Stress Intensity Factors for Several Contoured Double Cantilever Beam Specimens", Engg. Fracture Mech., 3, 1971.

5 CROSLEY, P.B. and RIPLING, E.J., "Dynamic Fracture Toughness of A533 Steel" Trans. of the ASME, J. of Basic Engg. September, 1969

Table I Circumferencial Mechanical Properties of Aged Zr-2.5Nb Tubing

TEMPERATURE (°C)	HYDROGEN CONTENT (ppm)	ULTIMATE STRENGTH (kg/mm^2)	0.2% PROOF STRESS (kg/mm^2)	ELONGATION (%)	REDUCTION IN AREA (%)
R. T.	0	87.7	79.4	18.8	48.5
	50	79.7	69.8	13.7	43.3
	300	73.6	62.7	12.1	32.4
300	0	59.7	—	18.0	64.0
	50	52.7	—	27.3	64.5
	100	52.3	—	21.1	63.0
	300	49.6	—	15.3	59.3

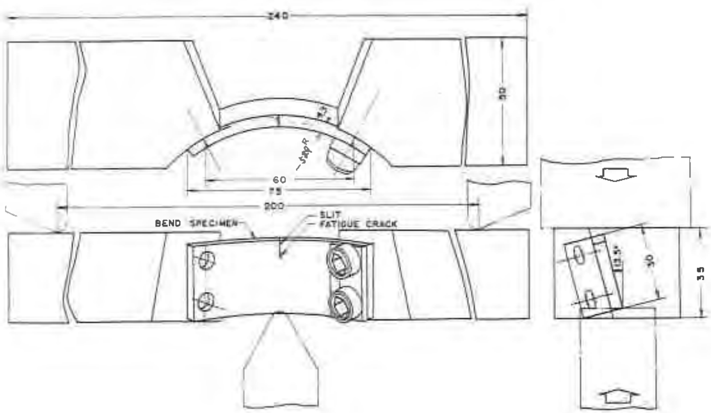

Fig 1 Construction of Specimen Assembly for Bending Test

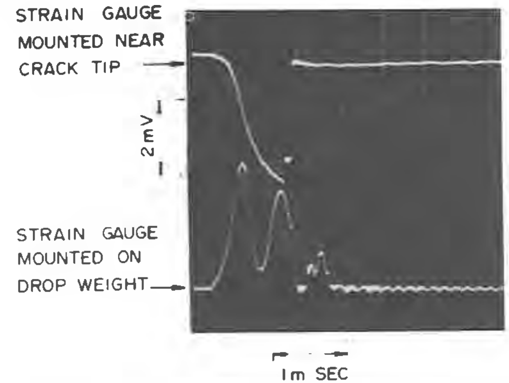

Fig.2 Typical load - time curve in dynamic fracture test

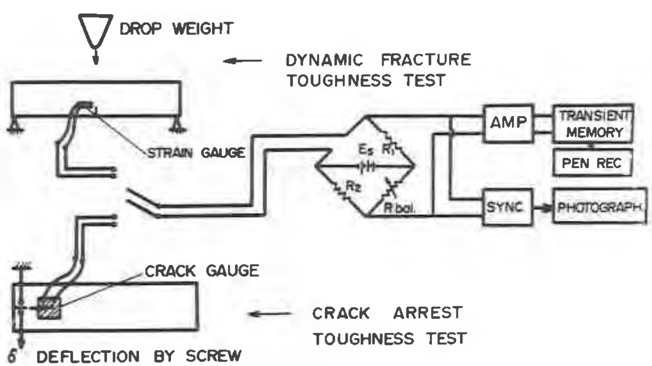

Fig.3 Block diagram of instrumentation of dynamic fracture toughness and crack velocity for crack arrest test

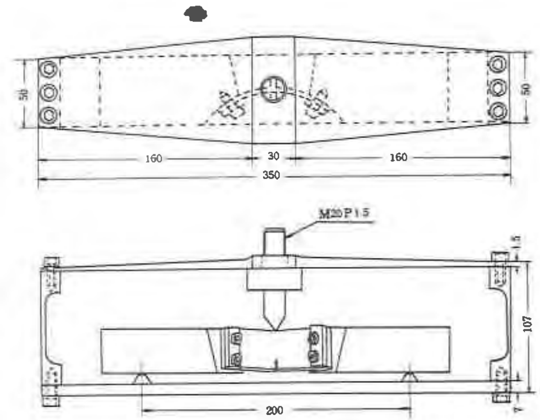

Fig. 4 Loading frame for H-enrichment under applid stress

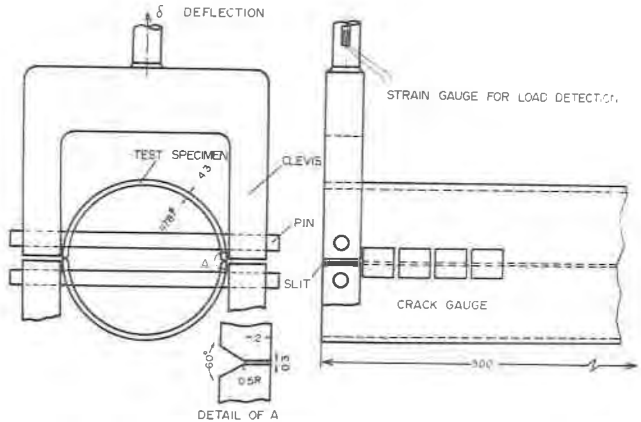

Fig 5 Construction of specimen assembly for crack arrest toughness test

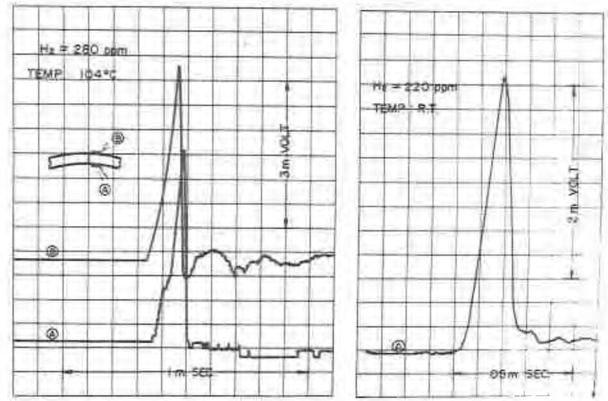

Fig.7 Typical time - load curve using strain gauge mounted near crack tip for dynamic fracture test

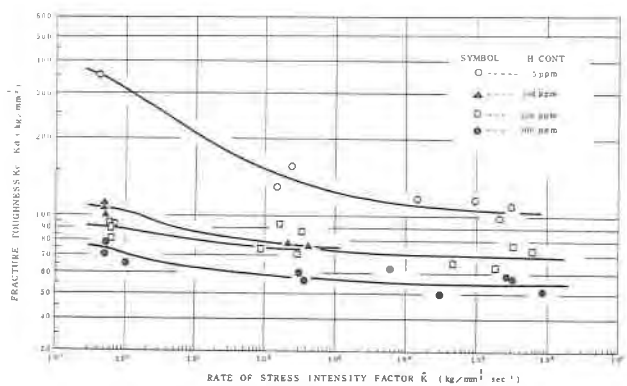

Fig. 6 Effect of strain rate on dynamic fracture toughness.

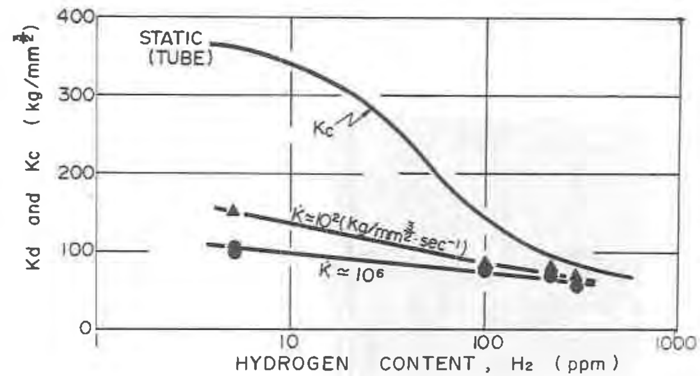

Fig. 8 Effect of hydrogen content on dynamic fracture toughness

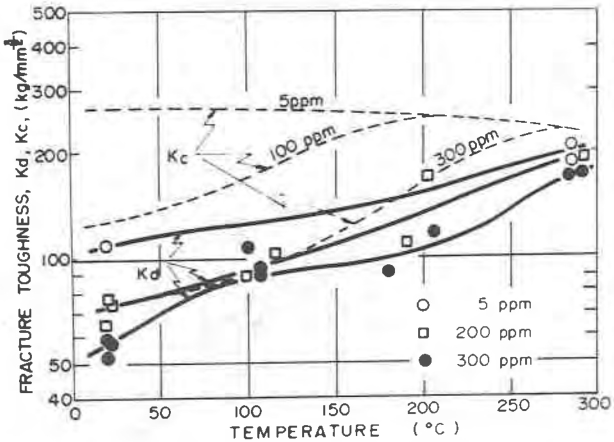

Fig.9 Effect of temperature on dynamic fracture toughness

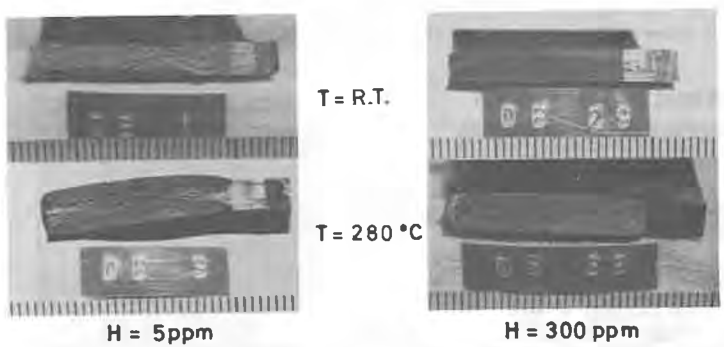

Fig. 10 Fracture surface appearance of dynamic fracture toughness test ($K=10^5\ kg/mm^{3/2}\cdot sec^{-1}$)

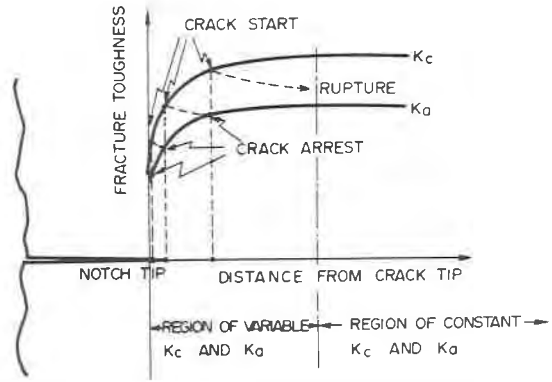

Fig.12 Fracture model of specimen being H-enriched under stress

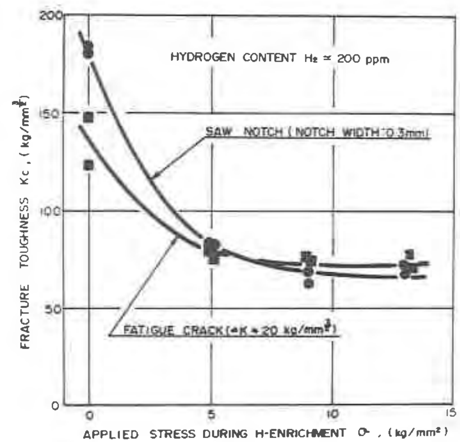

Fig.11 Effect of applied stress during hydrogen enrichment on fracture toughness

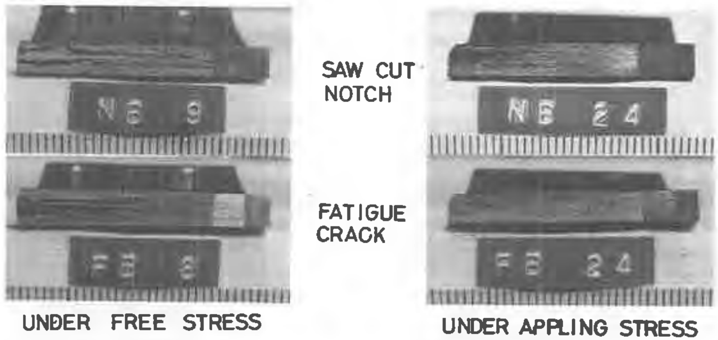

Fig. 13 Fracture surface appearance of specimen H-enriched under applid stress

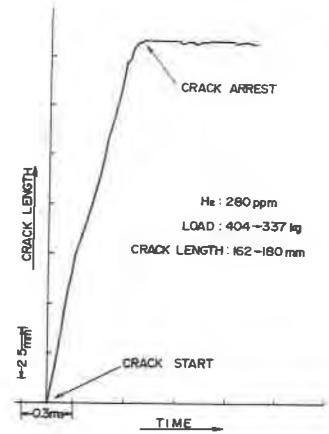

Fig.15 Typical brittle crack propagation behavior using crack gauge mounted in front of crack tip

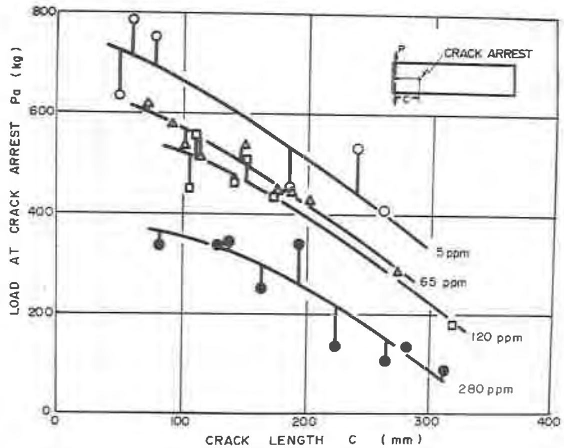

Fig.14 Brittle crack arrest strength of simulated DCB specimen

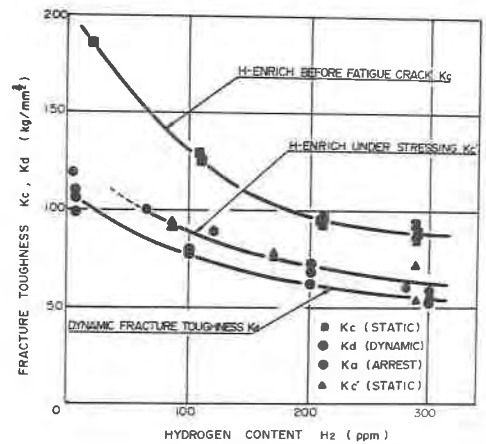

Fig.16 Effect of hydrogen content on static and dynamic fracture toughness and crack arrest toughness ($\dot{K} = 10^{5} \sim 10^{6}$ kg/mm$^{3/2}$ sec^{-1})